LETTERS

Charge Dependence of Surface Plasma Resonance on 2 nm Octanethiol-Protected Au Nanoparticles: Evidence of a Free-Electron System

Georgeta C. Lica, Brian S. Zelakiewicz, Mariana Constantinescu, and YuYe Tong*

Department of Chemistry, Georgetown University, 37th & O Streets, NW, Washington, D.C. 20057

Received: October 14, 2004; In Final Form: November 8, 2004

Charge dependence of surface plasma resonance (SPR) was investigated on 2 nm octanethiol-protected Au nanoparticles. Remarkably, if assuming that each Au-thiol bond localizes one free electron, the observed variations in peak position of the SPR bands as a function of charge can be precisely calculated by simple Mie theory without any adjustable parameters but by using the number of the remaining free electrons in the particle and the experimentally determined dielectric constant for the protecting layer of octanethiol. Additionally, the variations in line-width of the SPR bands can also be quantitatively described by the phenomenological damping law $\Delta\Gamma = Av_F/R$ with $A = 1.2$, a value that suggests a strong chemical-interface damping effect that is consistent with a strong metal−thiol bonding. In the calculations, Perdew's classic spherical jellium model is used to account for the electron spill-out effect. Altogether, these results not only strongly support recent findings by Dickson and co-workers (*Phys. Rev. Lett.* **2004**, *93*, 077402) who have shown that the nascent electronic properties of subnanometer Au nanoclusters are of free-electron characteristics but also provide much needed evidence of a continuation of a free-electron system into a particle size range where the collective plasmonic behavior has just emerged.

There has been a continuous interest,[1−16] with an increasing sophistication,[17] in understanding fundamentally the optical properties of metal nanoparticles, in particular the surface plasma resonance (SPR), since Faraday's seminal work in the middle of the 19th century.[18] The prevailing theories to interpret the SPR of metal nanoparticles of diverse morphologies are largely based on the Mie theory,[19] in which the response of spherical metal particles to an external electromagnetic excitation is solved electrodynamically under suitable boundary conditions. For spherical metal particles larger than 5 nm, strong SPR bands are usually observed and can, to a large extent, be quantitatively analyzed by Mie theory.[9,17] For smaller metal particles, however, consensus remains elusive. In particular, for alkanethiol-protected Au nanoparticles, it has been concluded that a simple extrapolation based on the bulk electronic properties does not lead to a quantitative Mie-theory interpretation of their SPR bands.[7] Indeed, an interesting yet apparently contradictory observation is that no viable SPR has been observed in sub-2 nm, ligand-protected Au nanoparticles[3,5,7] whereas strong SPR was detected in even smaller sodium clusters such as Na_8 to Na_{20}.[17] This has been seen as evidence showing the departure of the electronic properties of Au nanoparticles from a free-electron system describable by the spherical jellium model,[17] which is best represented by alkaline metal clusters.[20] However, Dickson and co-workers have very recently observed striking optical properties of Au quantum dots in the size range between Au_5 and Au_{31} and shown that they can be precisely described by the simple spherical jellium model.[21] That is, the nascent electronic properties of sub-nm Au nanoculsters are of free-electron characteristics.

In this paper, we present a quantitative analysis of the SPR bands of narrowly distributed, octanethiol-protected Au nanoparticles having an average particle size of 2 nm (Au_{247}) as a function of charge. The conclusions of the analysis are in agreement with those of Dickson et al.[21] but in a different particle size range. Specifically, the analysis started with an assumption that each strong metal−thiol bond localizes one free electron. Then, the number (N) of the remaining free electrons in a Au nanoparticle was calculated using the thiol coverage determined by thermogravimetric analysis. We have found that the variations in peak position of the SPR bands as a function of charge can be precisely calculated by using simple, free-electron based Drude-type Mie theory without any adjustable parameters if N is used for the number of free electrons in the particle and the experimentally determined dielectric constant of the octanethiol layer for that of surrounding medium. Moreover, the phenomenological damping law,[17] $\Delta\Gamma = Av_F/R$ (where $\Delta\Gamma$ is the line-width of the SPR band in frequency, A is the damping constant of order of unit, v_F is the Fermi velocity, and R is the radius of the particle) can also describe quantitatively the variations in line-width as a function of charge with $A = 1.2$. $A > 1$ is an indication of a strong chemical interface damping, which is consistent with the idea of a strong Au-thiol bonding. In all these calculations, the electron spill-out effect was taken into consideration by using Perdew's spherical jellium model.[22] These results not only confirm again the free-electron nature of the Au nanoparticles found previously[21] but also offer a very important piece of complementary information that

* Corresponding author. E-mail: yyt@georgetown.edu.

10.1021/jp045302s CCC: $27.50
Published on Web 11/25/2004

extends further in establishing a "road map" from the atomic properties toward those of the bulk for Au.

Experimentally, varying the number of free electrons offers a complementary way to test the jellium-model hypothesis other than the usual *R*-dependence investigations.[17] Our strategy is quite simple. The recently discovered quantized electrochemical double-layer charging of a metal particle ensemble,[23,24] the stability of the charged system after reaching charge equilibrium,[25] and its reversible redox-like property[26,27] enable us to vary *quantitatively* the number of free electrons residing on the particles *without* changing the particle size and the dielectric environment.[25] By doing so, the observed effects on the SPR can then be attributed mainly to changes in the electron density. To maximize the effect, the particle size needs to be as small as possible to the extent that the SPR profile should still be reasonably well-defined. We found that among the samples we have synthesized, the sample with a mean diameter of 2 nm represents the best compromise. Notice that charge dependences of SPR have been observed previously in both Ag[28] and Au[14] nanoparticles. However, no such quantitative analyses have yet been reported.

Our octanethiol-protected Au nanoparticles were prepared by the well-established two-phase approach pioneered by Schriffin and co-workers.[29] The details on our synthesis procedure can be found elsewhere.[30] Briefly, the $AuCl_4^-$ ions in an aqueous solution were first extracted completely into toluene via tetraoctylammonium bromide (TOAB) under vigorous stirring and the organic phase was separated thereafter. An appropriate amount of octanethiol determined by a Au/thiol ratio molar of 1:2 was then added to the separated, $AuCl_4^-$-containing organic phase. The reduction of Au ions was realized after a quick addition of abundant $NaBH_4$ solution to the organic phase under vigorous stirring, resulted in the formation of a dark brown Au colloid. The formed Au nanoparticles then went through several cycles of rotor evaporation, washing, precipitation, and filtering to remove the surfactant TOAB and any unreacted thiols, producing the brown black materials that are very stable in air, are redissolvable in organic solvents, and can be re-solidified by simple evaporation. The Au nanoparticles so synthesized show dominantly a spherical morphology, as demonstrated by the transmission electronic microscopy (TEM) measurements.[30] The cleanness of the product was always checked by routine ^1H and ^{13}C NMR.

Differential pulse voltammetry (DPV) and quantized double-layer charging were carried out on an EG&G 273A potentiostat (Princeton Applied Research) controlled by a PC with a CoreWare software package (Scribner) and utilizing a conventional three-compartment, three-electrode cell. Pt wires were used as both working and counter electrodes and Ag/AgCl (3 M) as a reference electrode. The compartments hosting the counter and reference electrodes containing only supporting electrolyte were separated from the working compartment through a Vycor membrane. Typically, 30 mg of octanethiol-protected Au nanoparticles was dissolved in 15 mL CH_2Cl_2 with 0.1 M Bu_4NClO_4 as a supporting electrolyte. The freshly prepared sample has an open circuit potential around −0.3 V with respect to Ag/AgCl (3 M). Figure 1A shows the DPV in which the stars indicate the redox charging waves and each wave corresponding to charging/discharging of the particles by one electron. Using the open circuit potential as a neutral state reference, the first peak positive to it was assigned a *z* (charge) value of +1 and the first one negative to it a value of −1, as indicated by the arrows in the figure. All other *z* values were assigned accordingly. It has been shown that the formal potential

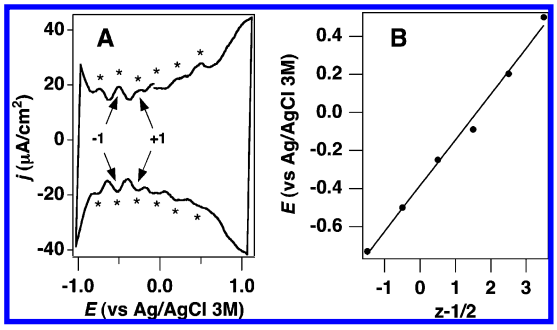

Figure 1. (A) DPV of the octanethiol-protected Au nanoparticles in a CH_2Cl_2 solution of 0.1 M Bu_4NClO_4. The stars indicate the redox-like charging peaks and the arrows show the assignment of the *z* values. (B) $E_{z,z-1}$ vs *z* plot by which the potential of zero charge, the capacitance, and the average particle size of the nanoparticle can be deduced. The straight line is a fit to eq 1.

of the charging peak for the "redox couple" $z/z-1$, $E_{z,z-1}$, can be expressed as a function of *z*:[26,27]

$$E_{z,z-1} = E_{pzc} + (e/C_{MPC})(z - 1/2) \quad (1)$$

where *e* is the electronic charge, E_{pzc} is the *p*otential of *z*ero *c*harge (i.e., the neutral species), and C_{MPC} is the integral capacitance of a *m*onolayer-*p*rotected metal *c*luster. The $E_{z,z-1}$ vs *z* plot is shown in Figure 1B, and the straight line is the fit to eq 1 with $E_{pzc} = -0.39 \pm 0.02$ V and $e/C_{MPC} = 0.24 \pm 0.01$ V. Thus, $C_{MPC} = 0.67$ aF. Approximating a monolayer-protected nanoparticle by a conducting sphere of radius *R* with a dielectric coating of thickness *d* and dielectric constant ϵ, one can show easily, by simple electrostatic reasoning,[26,27] that the capacitance of the sphere is

$$C_{MPC} = 4\pi\epsilon\epsilon_0 R(1 + R/d) \quad (2)$$

where ϵ_0 is the vacuum permittivity. Using $d = 1.02$ nm and $\epsilon = 3.2$ for octanethiol protecting layer,[30,31] eq 2 gives an *R* value of 1.0 nm that was used as the average particle size of the sample. The fact that almost equally spaced, well-resolved double-layer charging peaks were observed indicates that the sample has narrow size distribution (<15%), which was confirmed by TEM measurement.[30]

Two freshly prepared Au nanoparticle solutions were charged at −0.7 and +0.5 V, respectively, for 5 h under continuous Ar bubbling. The open circuit potentials of charged samples stabilized respectively at −0.48 and +0. 19 V, which correspond to *z* values of −1 and +3 according to Figure 1A. To check the long-term stability of the charged samples, a control experiment was done in which the solvent of a charged sample was evaporated. After being redissolved, the open circuit potential was found to be the same as that before evaporation. This observation is in agreement with those in ref 23, showing a quite robust charge stability of the samples. UV−vis spectra were taken on a Hitachi U-3501 double beam spectrophotometer with 1 cm optical path quartz cells immediately after the samples reached the equilibrium potential (approximately 30 min after stopping charging), i.e., −0.48 and +0.19 V, respectively. The sample concentrations were diluted from the initial concentration by 8−10 times and wavelength calibration and baseline collection with CH_2Cl_2/0.1 M Bu_4NClO_4 were performed prior to each set of measurements. The corresponding spectra are shown in Figure 2A, together with that of an uncharged sample (each spectrum contains 351 data points). A SPR can be clearly discerned at about 500 nm, a value characteristic for gold nanoparticles.

TABLE 1: Fitting Parameters to Eq 3 for UV−Vis Spectra in Figure 3

charges	a	b (10^{-5}, nm^{-1})	c	λ_0 (nm)	$\Delta\lambda$ (=2.36 σ)/ λ_0^2 (10^{-6}, nm^{-1})
−1	7.84 ± 0.01	434.8 ± 0.4	0.199 ± 0.001	505.8 ± 0.2	690 ± 5
0	10.12 ± 0.01	424.4 ± 0.4	0.257 ± 0.001	508.3 ± 0.2	680 ± 5
+3	13.05 ± 0.02	444.7 ± 0.5	0.318 ± 0.001	510.4 ± 0.2	667 ± 6

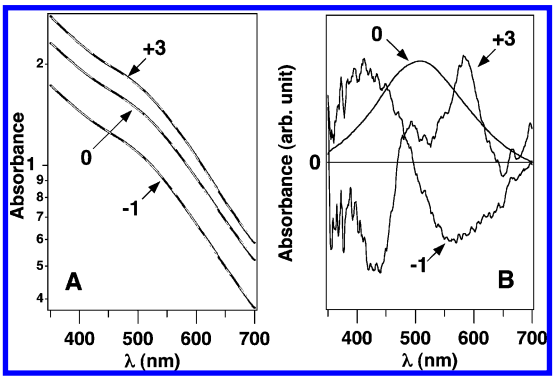

Figure 2. (A) UV−Vis spectra of negatively, positively, and uncharged Au nanoparticles. The dash−dotted white lines are the fits to eq 3 and the corresponding fitting parameters are collected in Table 1. (B) Representative normalized Gaussian-like surface plasma resonance peak after subtraction of the exponentially decay background (see text for details) for the uncharged sample and the difference spectra (×40) with respect to the former for the other two as indicated by the arrows. The blue and red shifts with respect to the uncharged sample are clearly discernible.

The line shape of a SPR in classic Mie theory is a Lorentzian.[17] However, it has been observed previously that a Lorentzian actually cannot describe well the line shape of SPRs from ligand-protected, very small Au nanoparticles.[7] On the other hand, it has also been concluded experimentally that an exponentially decaying absorption function is a characteristic background behavior for embedded Au clusters having size from 1 to 2 nm which is caused mainly by the 5d to 6sp interband transitions.[3,5,17] For our case, we found that the total absorption curves can be very well represented by

$$A(\lambda) = a\exp(-b\lambda) + c\exp[-(\lambda-\lambda_0)^2/2\sigma^2] \qquad (3)$$

where a, b, c, λ_0, and σ are fitting parameters. The first exponentially decaying term represents the background of the interband transition whereas the second Gaussian term represents the SPR with λ_0 as the peak position and $\Delta\lambda = 2.36\sigma$ as the full width at half-maximum (fwhm). The fitted curves are shown as the dash−dotted white lines in Figure 2A, and the corresponding parameters are collected in Table 1. It is interesting to note that if, instead of the Gaussian, a Lorentzian is used, then the quality of fitted curves become much worse, reminiscent of the previously published results.[7] Although it is not clear at this moment why the SPR profile from ligand-protected, very small Au nanoparticles has a more Gaussian- than Lorentzian-like line shape, eq 3 can, nevertheless, enable well-defined peak positions and line-widths to be extracted for our analysis. Notice that the exponential decay constants obtained from the fits are very close to the previously known value (340×10^{-5} nm^{-1})[3] and almost the same among themselves. Additionally, the ratio a/c is also a constant for the three fits, suggesting a decoupling of the 5d to 6sp interband transitions from the SPR. These results strongly indicate that the peak positions and line-widths extracted by using eq 3 are physically sound and meaningful. By subtracting the exponentially decaying component from the measured UV−vis spectra, normalized remaining Gaussian lines were obtained, as represented by the one of the uncharged sample shown in Figure 2B. The difference spectra (amplified by 40 times) with respect to that of the uncharged one are also shown for the charged samples to demonstrate clearly the changes in the peak positions caused by the electrochemical charging. It can be seen unambiguously from the difference spectra that the positive (negative) charging indeed red (blue) shifts the SPR with respect to that of the uncharged sample. This is in good agreement with previous observations.[14,28]

For very small metal nanoparticles as the ones studied here, the effect of electron spill-out becomes important and can no longer be neglected.[17] According to Perdew's classic spherical jellium model,[22] the effective radius (in unit of nm) of the free electrons in a spherical nanoparticle having a radius of R_0 is

$$R = R_0 + 0.0529 \times \left[5.207\left(\frac{R_0}{N^{1/3}}\right)^{-3/2} - 7.415\left(\frac{R_0}{N^{1/3}}\right)^{-1} + 4.874\left(\frac{R_0}{N^{1/3}}\right)^{-1/2}\right] \qquad (4)$$

where N is the number of free electrons on the particle. The second part in eq 4 accounts for the electron spill-out that depends on the number of free electrons on the particle. On the other hand, according to Mie theory, the SPR peak position λ_0 as a function of the number of charged electrons, x, can be expressed as[17]

$$\lambda_0 = \sqrt{\frac{16}{3}\pi^3 R^3 \frac{m_e c^2}{e^2}\epsilon_0}\frac{\sqrt{1+2\epsilon}}{\sqrt{N_0 - x}} \qquad (5)$$

where m_e is the mass of electron, c is the speed of light, and N_0 is the number of free electrons in an uncharged particle. All other parameters are defined in eqs 1 and 2. Notice that for the octanethiol-protected 2 nm Au nanoparticles, the effect of the solvent refractive index can be safely neglected and ϵ becomes that of the octanethiol layer.[14] Now for a Au nanoparticle of size $2R_0 = 2$ nm, the total Au atoms can be estimated by

$$N_{\text{total}} = \frac{2\pi}{3}\left(\frac{2R}{a}\right)^3 \qquad (6)$$

where $a = 0.408$ nm is the lattice constant of bulk Au. Thus, $N_{\text{total}} = 247$. Assuming an ideal cubooctahedron morphology, the number of surface Au atoms can also be deduced:[32] $N_{\text{surf}} = 139$. The thermogravimetric analysis of the sample shows a molar ratio of 0.34 between thiol and Au. A coverage of 61% can thus be deduced, which is in close agreement with the previously published value: 66%.[33] If each Au−thiol surface bonding localizes one free electron, then the number of the remaining free electrons $N_0 = 247 - 85 = 162$. Using this value, together with $R_0 = 1$ nm and $\epsilon = 3.2$,[30] the solid line shown in Figure 3A was obtained by using eq 5 in which R is replaced with eq 4. It is indeed remarkable that the results calculated with eq 5 without any adjustable parameters can fit the experimental data so well, which is a strong indication showing that Au nanoparticles are largely a free electron system. A note of caution, however, is that eq 4 was derived for a "naked-surface" jellium sphere whereas the system dealt with here is octanethiol-protected metal nanoparticles. Nonetheless, because

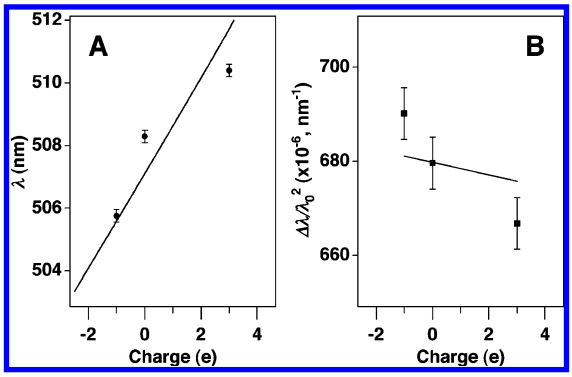

Figure 3. (A) Surface plasma peak position λ_0 as a function of charge. The solid line is calculated with eq 5 without an adjustable parameter. (B) Full width at the half-maximum amplitude $\Delta\lambda/\lambda_0^2$ as a function of charge. The solid line is a one-parameter fit to eq 7 that gives $A = 1.2$.

the effect of adsorbates on the electronic "spill-out" is mainly through the change of the work function,[34] which has already been taken into account by the reduction in the number of the free electrons as discussed above, we believe that a direct use of eq 4 in eq 5 is well justified.

Another important parameter in the SPR is the so-called relaxation frequency $\Delta\Gamma$ that determines the broadness of the resonance peak. For particles as small as ours, it can, according to the phenomenological damping law,[17] be expressed as $\Delta\Gamma = A(\upsilon_F/R) \approx 2\pi c(\Delta\lambda/\lambda_0^2)$, where A is the line-broadening constant and υ_F is the Fermi velocity of the free electrons[17] and $\Delta\lambda = 2.36\sigma$ is the fwhm in nm (not in frequency, vide supra). Although the true physical meaning of the A constant is certainly not free of debate,[35] it is, however, reasonable to conclude that $A > 1$ indicates a strong chemical interface damping effect.[17] Figure 3B presents the $(\Delta\lambda/\lambda_0^2)$ vs charge plot. With a Drude-type free-electron model for υ_F,[36] it can be shown that

$$\frac{\Delta\lambda}{\lambda_0^2} = A\left(\frac{9}{256\pi^5}\right)^{1/3}\frac{h}{m_e c R^2}(N_0 - x)^{1/3} \qquad (7)$$

where h is the Plank constant. Using $N_0 = 162$, the data in Figure 3B are fitted to eq 7 with A as the *only* fitting parameter, as shown by the solid line in the figure. Remarkably, the A value obtained from the fit is 1.2 and again compares very favorably with the available literature values under similar circumstances.[17] It is worth noting that eq 7 accounts quantitatively for *all* the line-broadenings within a margin of less than 5% and the fact that $A > 1$ is consistent with a strong metal−thiol bonding interaction.

Finally, it is important to point out that the free-electron based eq 5 neglects any possible influences from the d electrons, which are believed to significantly complicate the free-electron nature of noble metals that include Au.[37,38] Although our results show clearly a physically meaningful continuation from those of Dickson et al.[21] in terms of the free-electron characteristics in Au nanoparticles, one challenging issue is that eq 5 leads to the Drude SPR frequency when $R \rightarrow \infty$ instead of the experimentally observed frequency which is much smaller. The conventional interpretation of such a red shift of the SPR is that the nonnegligible polarization of the d electrons in the noble metals screens significantly the s electrons and, therefore, causes the observed reduction in the SPR frequency with respect to that predicted by the free-electron model.[39] The blue shift of the SPR observed in free cationic silver clusters Ag_n^+ (n = 5−70)[40] and the opposite red shift observed in free anionic Ag_n^- (n = 6−20)[41] as n decreases have been rationalized in the same vein in that a reduced s−d screening was thought to be responsible for the former and an enhanced one for the latter. It is particularly interesting to notice that the enhanced s−d screening expected for the anionic Ag_n^- according to the d-electron polarization model also accounts for the observed red-shift for a given n (i.e., a given cluster size) due to an increase in the negative charge.[41] Yet, an opposite blue shift was observed as the Au nanoparticles become more negatively charged in our case (infra supra). This *qualitatively* different trend strongly indicates that the d electron polarization, if any, cannot be a dominant factor in the octanethiol-protected Au nanoparticles studied here, justifying again the free-electron description of the system. It is possible that as the particle size grows bigger, the polarizability of the d electrons may increase. Consequently, the d electrons become more influential in determining the optical properties of Au. Clearly, more investigations are warranted.

In summary, by using a quantized electrochemical double-layer charging method, a charge dependence of SPR was investigated on the octanethiol-protected Au nanoparticles having an average particle size of 2 nm. Most remarkably, the observed shift in the SPR peak position and the variation in the corresponding line width as a function of charge can be well rationalized in a quantitative and self-consistent way by simple free-electron based Mie theory and the phenomenological damping law in which the effect of electron spill-out was taken into consideration with Perdew's classic spherical jellium model. These results are important because (1) they provide strong evidence of the free-electron nature of the Au nanoparticles studied here, (2) they highlight the important role of the metal−ligand bonding in determining the SPR characteristics in these metal nanoparticles, (3) they may suggest the potential applicability of Mie theory to charged nanoparticles, and (4) they may offer a new way to estimate the thiol coverage.

Acknowledgment. This work was partially supported by a PRF G-type grant, by a Georgetown Star-up fund, and by a Pilot Research Project Grant as well as a Summer Research Grant from the Georgetown Graduate School.

References and Notes

(1) Doyle, W. T. *Phys. Rev.* **1958**, *111*, 1067−1072.
(2) Doremus, R. H. *J. Chem. Phys.* **1965**, *42*, 414−417.
(3) Kreibig, U.; Frauth, K.; Granqvist, C.-G.; Schmid, G. *Z. Phys. Chem.* **1990**, *169*, 11−28.
(4) Creighton, J. A.; Eadon, D. G. *J. Chem. Soc., Faraday Trans.* **1991**, *87*, 3881−3891.
(5) Duff, D. G.; Baiker, A.; Edwards, P. P. *J. Chem. Soc., Chem Commun* **1993**, 96−98.
(6) Mulvaney, P. *Langmuir* **1996**, *12*, 788−800.
(7) Alvarez, M. M.; Khoury, J. T.; Schaaff, T. G.; Shafigullin, M. N.; Vezmar, I.; Whetten, R. L. *J. Phys. Chem. B* **1997**, *101*, 3706−3712.
(8) Schaaff, T. G.; Shafigullin, M. N.; Khoury, J. T.; Vezmar, I.; Whetten, R. L.; Cullen, W. G.; First, P. N. *J. Phys. Chem. B* **1997**, *101*, 7885−7891.
(9) Kelly, K. L.; Coronado, E.; Zhao, L. L.; Schatz, G. C. *J. Phys. Chem. B* **2003**, *107*, 668−677.
(10) Félidj, N.; Aubard, J.; Lévi, G. *J. Chem. Phys.* **1999**, *111*, 1195−1208.
(11) Schaaff, T. G.; Shafigullin, M. N.; Khoury, J. T.; Vezmar, I.; Whetten, R. L. *J. Phys. Chem. B* **2001**, *105*, 8785−8796.
(12) Prodan, E.; Radloff, C.; Halas, N. J.; Nordlander, P. *Science* **2003**, *302*, 419−422.
(13) Henglein, A.; Linnert, T.; Mulvaney, P. *Ber. Bunsen-Ges. Phys. Chem.* **1990**, *94*, 1449−1457.
(14) Templeton, A. C.; Pietron, J. J.; Murray, R. W.; Mulvaney, P. *J. Phys. Chem. B* **2000**, *104*, 564−570.
(15) Pinchuk, A.; Kreibig, U.; Hilger, A. *Surf. Sci.* **2004**, *557*, 269−280.
(16) Toyota, A.; Nakashima, N.; Sagara, T. *J. Electroanal. Chem.* **2004**, *565*, 335−342.

(17) Kreibig, U.; Vollmer, M. *Optical Properties of Metal Clusters*; Springer-Verlag: New York, 1995; Vol. 25.
(18) Faraday, M. *Philos. Trans. R. Soc. London* **1857**, *147*, 145−181.
(19) Mie, G. *Ann. Phys.* **1908**, *25*, 377.
(20) Heer, W. A. d. *Rev. Mod. Phys.* **1993**, *65*, 611−676.
(21) Zheng, J.; Zhang, C.; Dickson, R. M. *Phys. Rev. Lett.* **2004**, *93*, Art. No. 077402.
(22) Perdew, J. P. *Phys. Rev. B* **1988**, *37*, 6175−6180.
(23) Ingram, R. S.; Hostetler, M. J.; Murray, R. W.; Schaaff, T. G.; Khoury, J. T.; Whetten, R. L.; Bigioni, T. P.; Guthrie, D. K.; First, P. N. *J. Am. Chem. Soc.* **1997**, *110*, 99279−9280.
(24) Chen, S.-W.; Ingram, R. S.; Hostetler, M. J.; Pietron, J. J.; Murray, R. W.; Schaaff, T. G.; Khoury, J. T.; Alvarez, M.; Whetten, R. L. *Science* **1998**, *280*, 2098−2101.
(25) Song, Y.; Murray, R. W. *J. Am. Chem. Soc.* **2002**, *124*, 7096−7102.
(26) Weaver, M. J.; Gao, X.-P. *J. Phys. Chem.* **1993**, *97*, 332−338.
(27) Chen, S.-W.; Murray, R. W.; Feldberg, S. W. *J. Phys. Chem. B* **1998**, *102*, 9898−9907.
(28) Henglein, A.; Mulvaney, P.; Linnert, T. *Faraday Discuss.* **1991**, 31−44.
(29) Brust, M.; Walker, M.; Bethell, D.; Schiffrin, D. J.; Whyman, R. *J. Chem. Soc., Chem. Commun.* **1994**, 801−802.
(30) Lica, G. C.; Zelakiewicz, B. S.; Tong, Y. Y. *J. Electroanal. Chem.* **2003**, *554*−*555*, 127−132.
(31) Hicks, J. F.; Templeton, A. C.; Chen, S.; Sheran, K. M.; Jasti, R.; Murray, R. W.; Debord, J.; Schaaff, T. G.; Whetten, R. L. *Anal. Chem.* **1999**, *71*, 3707−3711.
(32) Van Hardeveld, R.; Hartog, F. *Surf. Sci.* **1969**, *15*, 189−230.
(33) Terrill, R. H.; Postlethwaite, T. A.; Chen, C.-H.; Poon, C.-D.; Terzis, A.; Chen, A.; Hutchison, J. E.; Clark, M. R.; Wignall, G.; Londono, J. D.; Superfine, R.; M. Falvo; Johnson, C. S., Jr.; Samulski, E. T.; Murray, R. W. *J. Am. Chem. Soc.* **1995**, *117*, 12537−12548.
(34) Feibelman, P. J.; Hamann, D. R. *Surf. Sci.* **1985**, *149*, 48−66.
(35) Hövel, H.; Fritz, S.; Hilger, A.; Kreibig, U.; Vollmer, M. *Phys. Rev. B* **1993**, *46*, 18178−18188.
(36) Aschroft, N. W.; Mermin, N. D. *Solid State Physics*; W. B. Saunders Co.: Philadelphia, 1976.
(37) Liebsch, A. *Phys. Rev. Lett.* **1993**, *71*, 145−148.
(38) Palpant, B.; Prével, B.; Lermé, J.; Cottancin, E.; Pellarin, M.; Treilleux, M.; Perez, A.; Vialle, J. L.; Broyer, M. *Phys. Rev. B* **1998-I**, *57*, 1963−1970.
(39) Liebsch, A. *Phys. Rev. B* **1993**, *48*, 11317−11328.
(40) Tiggesbäumker, J.; Köller, L.; Meiwes-Broer, K. H.; Liebsch, A. *Phys. Rev. A* **1993**, *48*, R1749−R1752.
(41) Tiggesbäumker, J.; Köller, L.; Meiwes-Broer, K. H. *Chem. Phys. Lett.* **1996**, *260*, 428−432.